Reduction of pTau and APP Levels in Mammalian Brain After Low-Dose Radiation

Diego Iacono (diego.iacono.ctr@usuhs.edu)
Uniformed Services University https://orcid.org/0000-0001-5511-0950
Erin Murphy
Uniformed Services University
Soundarya Avantsa
Uniformed Services University
Daniel Perl
Uniformed Services University
Regina Day
Uniformed Services University

Article

Keywords: Brain radiation, Tau phosphorylation, Amyloid Precursor Protein, Neosynaptogenesis, Neuroplasticity, Radiotherapy for Neurodegenerative Disorders

Posted Date: August 4th, 2020

DOI: https://doi.org/10.21203/rs.3.rs-48631/v1

Version of Record: A version of this preprint was published at Scientific Reports on January 26th, 2021. See the published version at https://doi.org/10.1038/s41598-021-81602-z.

Abstract

Brain radiation can occur from treatment of brain tumors or accidental exposure. Brain radiation has been rarely considered, though, as a possible tool to alter proteins involved in neurodegenerative disorders. We analyzed molecular and neuropathology changes of phosphorylated-Tau (pTau), all-Tau forms, β-tubulin, amyloid precursor protein (APP), glial fibrillary acidic protein (GFAP), ionized calcium binding adaptor molecule 1 (IBA-1), myelin basic protein (MBP), and GAP43 in Frontal Cortex (FC), Hippocampus (H) and Cerebellum (CRB) of swine brains 4 weeks following total-body radiation (1.79 Gy). Radiated-animals showed lower levels of pTau in FC and H, APP in H and CRB, GAP43 in CRB, and higher level of GFAP in H vs. sham-animals. These changes were not accompanied by obvious neurohistological changes, except for astrogliosis in the H. These findings are novel, and might open new perspectives on brain radiation as a therapeutic tool for interfering with the pathogenesis of various neurodegenerative disorders.

Introduction

Radiation-induced brain injury due to fractionated or single dose radiotherapy can generate a complex series of acute[1–3] and chronic changes[4,5], where the resulting clinical severity and therapeutic outcomes depend on the nature of the brain pathology involved (primary brain tumor vs. brain metastases), general medical conditions (older vs. younger patients), radiation techniques used (fractionated vs. single dose), requirement of isolated or combined chemotherapy+radiotherapy (isolated radiotherapy vs. antiblastic+radiation therapy), and total dose of *γ*-rays administered (low- vs. high-dose).

Generally, the central nervous system (CNS), and more specifically the brain, can be the target organ for radiation for medical purposes (e.g. treatments for primary brain tumors or palliative cures for cerebral metastatic neoplasia) or be one of the vital organs injured by nuclear power accidents, accidental nuclear contamination or nuclear war/attack[6–8]. Although brain radiation has been demonstrated to be useful in treating different types of brain tumors, especially when combined with other types of therapies[9,10], short- and long-term molecular and neuropathological effects of radiation on normal brain tissue are not completely understood yet[11–14].

Systematic neuropathological investigations using modern molecular protocols (e.g. quantification of Western blotting [WB]) and immunohistochemistry-based neurohistological techniques (e.g. polymers-based immunohistochemistry method) to examine the possible consequences of low-dose brain/total-body radiation (e.g. ~2.0 Gy) on large mammalian brains under normal (non-transgenic) anatomo-physiological conditions are currently inadequate[15–17]. In fact, the majority of the previous neuropathological studies have principally focused on brain tissues obtained from rodents[18–20] or from surgically resected human specimens after radiation and chemotherapy treatments[21], or have employed simplified experimental models such as neuronal or glial cells cultures[22–24]. However, higher order mammals such as swine have much more similar metabolic, cognitive and behavioral capacities to humans than rodents. Specifically, those higher cognitive and behavioral capacities are indeed the ones more frequently affected by long-term effects of brain radiation in humans[25]. Nonetheless, the relevance of a more systematic approach into investigating the effects of radiation on large mammalian brains originates from the clinical evidence that brain radiation can generate significant and often delayed (>6 months/years) neurological consequences (e.g. cognitive impairment, mood disorders, sleep disorders) in predisposed subjects[26]. These subjects are frequently children who underwent brain radiation as part of their treatment for either primary or secondary brain tumors[27–32]. Unfortunately, these types of treatments can have deleterious consequences on the normal brain tissue contiguous to the pathological targeted lesions. Surprisingly, though, very little is known about the possible beneficial effects of brain radiation in the realm of the various misfolded proteins (for example, Tau protein) involved in the pathomechanisms of various neurodegenerative disorders in humans.

Brain molecular analyses (e.g. precise measurements of different protein expression levels across different neuroanatomical regions) and their corresponding neuropathological effects examined in a large mammalian brain (e.g. swine) after few weeks post-radiation (e.g. 4 weeks) could greatly help in elucidating some of the earlier molecular events associated with different types of late neurological sequelae. These sequelae, among others, include neuroinflammatory and demyelination phenomena,

which are often observed during the later phases of the post-radiation natural progression in those subjects exposed to brain radiation for either medical or non-medical reasons[33,34]. Moreover, a better understanding of the post-radiation molecular and neuropathological changes in normal large mammalian brain tissue could also considerably contribute to identifying more effective prophylactic options that could be used in either clinical or nuclear environmental contamination/attack settings. Finally, low-dose brain radiation could prove to be actually beneficial in those brain conditions characterized by pathological accumulations of extra- or intra-cellular misfolded proteins such as *β*-amyloid and hyperphosphorylated-Tau lesions in Alzheimer's disease (AD), α-synuclein-positive Lewy bodies in Parkinson's disease (PD) or misfolded prion protein in Creutzfeldt–Jakob disease (CJD)[35]. In this study, we aim to analyze some possible molecular changes induced by low-dose total body radiation on the normal large mammalian brain that could be beneficial in the context of misfolded proteins-related neurodegenerative disorders. We meant to fill this gap of knowledge through the following aims:

1) identify early (4 weeks post-radiation) molecular brain alterations such as changes of soluble proteins expression levels [e.g. phosphorylated-Tau (pTau), all-forms of Tau, amyloid precursor protein (APP), glial fibrillary acidic protein (GFAP), ionized calcium binding adaptor molecule 1 (IBA–1), myelin basic protein (MBP), and neosynaptogenic markers (e.g. GAP43)], in large mammalian brains (e.g. swine brains) after a low-dose total-body radiation;

2) observe if different regions of a large mammalian brain (e.g. frontal cortex [FC], hippocampus [H] and cerebellum [CRB]) could differentially react by expressing different levels of those considered proteins when measured at an identical post-radiation time-point;

3) verify if a specific compound, for example captopril - a commonly prescribed angiotensin converting enzyme (ACE) inhibitor for the treatment of hypertension—which has been shown to provide improvement for some of the post-radiation neuropathological side effects in mice (e.g. brain microhemorrhages, hematopoietic injuries)[36] - might also have possible beneficial or prophylactic advantages when used in larger mammalian brains.

Results

Post-radiation general conditions

Based on the approved criteria for early euthanasia (recumbence with failure to gain standing posture, severe lethargy, and/or ataxia), two animals from the Radiation+Vehicle group were euthanized prior to the study end point due to radiation injuries, one at 19 days (for lethargy) and another at 20 days (for lethargy) post-radiation. The remaining animals, sham- (SH-) and radiated (RAD-) animals were euthanized at 33–35 days post-radiation and demonstrated no signs of illness. No significant difference in body weight was demonstrated between SH- and RAD-animals across the entire study time course (baseline: SH = 27.5 vs RAD = 22.9; Day 16: SH = 32.6 vs RAD = 29.4; Day 30: SH = 35.6 vs RAD = 35.9; weights expressed in pounds) (*see Supplementary Figure 1).*

Effect of Captopril Treatment

Interestingly, we found no statistically significant differences between captopril and vehicle treatment in all examined brain regions. Due to this outcome, captopril and vehicle treated groups were pooled together for further molecular analyses. Statistical analyses are described in the methods section.

Protein expression levels

Our results show that phosphorylated-Tau levels (CP13) were lower in RAD- vs. SH-animals in the FC ($p = 0.0187$, df = 20) and H ($p = 0.0388$, df = 20) regions (*Figure 1).*. Moreover, HT7 (all-Tau forms) and *β*-tubulin levels did not differ across any of the examined neuroanatomical regions (FC, H, CRB) (*Figure 2).*. Furthermore, APP protein expression level was lower in RAD- vs. SH-animals in the H ($p = 0.0009$, df = 20) and CRB region ($p = 0.0039$, df = 17) (*Figure 3A).*. In addition, unexpectedly, GAP43 expression level in the CRB was lower in RAD- vs. SH-animals as well ($p = 0.0051$, df = 17) (*Figure 3B).*.

By contrast, GFAP expression level was higher in RAD- vs. SH-animals in the H region (p = 0.007, df = 20). In addition, only in the FC region, an increase of DNA polymerase-β in RAD- vs. SH-animals (p = 0.0019, df = 20) was found (*Figure 4).*.

IBA–1 and MBP expression levels did not differ between RAD- vs. SH-animals in any of the examined brain regions. Finally, the measured expression levels of all phosphorylation-related enzymes (GSK3β, pGSKβ [Y216], PP2A-βa) did not differ in RAD- vs. SH-animals in any examined region (*Supplementary Figures 2–4).*.

Immunohistochemistry and Neurohistology outcomes

Immunohistochemistry protocols for CP13, HT7, APP, IBA–1, GFAP and MBP did not show any pathological accumulation of insoluble intra- (e.g. pTau neurofibrillary tangles-like lesions) or extra-cellular proteins (e.g. APP-positive DAI lesions) in RAD- vs. SH-animals (*Figure 5).* However, initial astroglial reaction (as assessed by HE satin and GFAP immunostain) was present in the H of RAD- vs. SH-animals (*Figure 6),,* specifically in the peri-dentate gyrus (peri-DG) area. HE, LFB, and CV stains did not show any intraparenchymal or necrotic-ischemic vascular lesions (including microhemorrhages) (HE), obvious myelin loss (LFB) or any evident nuclear or perinuclear damage (CV).

Discussion

The mammalian CNS, particularly the brain, represents an important target-organ that might be injured following radiation exposure (e.g. iatrogenic origins, nuclear accidents, war/terrorist attacks) resulting in a drastic reduction of either survival or long-term quality of life. The detrimental effects of brain radiation exposure might occur despite the implementation of preventative measures (as in the clinical setting) or prophylactic protocols (as after radiation contamination due to nuclear disaster or attack)[1,2]. While most radiation research investigations focus on minimizing long-term neurological consequences in the context of specific radiotherapy protocols (for example, using low-dose fractionated radiation for primary brain tumors) or on looking for prophylactic tools to minimize systemic injurious effects of radiation (e.g. using a compound such as captopril immediately after radiation), few studies have actually investigated the possible role of low-dose brain radiation to beneficially interfere with pathological processes occurring in neurodegenerative disorders such as Alzheimer's disease (AD) for example - a disorder associated with pathological accumulation of intracellular (pTau) and extracellular (β-amyloid) misfolded proteins across different vulnerable regions of the brain[37]. Interestingly, though, a recent study in transgenic rodents described reduction of β-amyloid plaque loads in the radiation-treated animals[38]. However, no earlier pTau or APP expression level changes across different brain regions have ever been described after a low-dose of total-body radiation using a large normal mammalian brain.

We have focused on the identification of some possible early molecular (protein expression level changes) and neuropathological consequences of low-dose total-body radiation (1.79 Gy total dose, which is a dose comparable to the ones commonly administered in the current radiotherapeutics protocols for brain tumors) after a relatively short period of time (~ 4 weeks) in a large mammalian brain (swine), and we have measured:

1. Lower levels of pTau (CP13) in the FC and H region of RAD- vs. SH-animals;
2. Lower levels of APP and GAP43 in the CRB of RAD- vs. SH-animals;
3. Higher level of GFAP in the H of RAD- vs. SH-animals;
4. Higher level of DNA-polymerase-β in the FC of RAD- vs. SH-animals.

No significant changes were found in microglial activation signals (as detected by either soluble IBA–1 levels or immunohistochemistry/morphological changes) or loss of myelin (as detected by levels of soluble MBP or through LFB stain assessment). Importantly, these findings on early molecular changes in a normal (non-transgenic) large mammalian brain in the absence of obvious neurohistological changes or brain lesions support the hypothesis that early specific molecular changes occur and are detectable after 4 weeks post-radiation across different brain regions exposed to the same fractionated low-dose of total-body radiation. Remarkably, the lower levels of pTau, APP and GAP43 observed across the different examined regions of the swine brain were not associated with apparent histological or morphological changes or activation signs of

microglial cells or demyelination phenomena, which are two processes normally observed at a later stage during the progression of the post-radiation process (>6 months/years after post-radiation)[33]. In addition, these novel findings show that the neuroanatomical regions involved in radiation-induced reduction of the examined protein expression levels are not uniformly altered along the same direction across different regions of the brain. Rather, these new data indicate a cellular response that involves different brain regions at different degrees and rates of changes along the varying post-radiation time points. This differential post-radiation timing is likely due to the intrinsic radiosensitivity to *γ*-rays in each specific cerebral region (based, for example, on their intrinsic genetically-determined metabolic rate) as well as possibly related to the total radiation dose administered[39–41]. These differential radiosensitivity-related aspects across different brain regions as well as their possible controlled modulation could lead to precise and effective neuroanatomical-based brain radiation protocols selectively tuned for a specific region of the brain, or a group of disease-related neuroanatomical regions, in the context of a specific brain disease and local brain tissue vulnerability.

Notably, the reduction of pTau levels induced by total-body radiation was observed in the absence of corresponding significant changes of all-Tau forms (HT7) across all the examined regions. The unchanged levels of total-Tau protein were also indirectly confirmed by the unchanged levels of *β*-tubulin (*Figure 2)*,, a protein strictly associated with Tau for the stabilization of microtubules[42]. It appears that one of the early effects of the low-dose radiation on intracellular Tau levels is the change of the ratios between phosphorylated and dephosphorylated forms. Intriguingly, the observed phenomenon of decreased pTau levels induced by low-dose radiation contrasts with the opposite phenomenon observed in AD pathogenesis (and other tauopathies), where a progressive process of Tau hyperphosphorylation is instead associated with increased levels of insoluble pTau and consequent accumulation in neurons and astroglial cells across the cerebral cortex[43,44]. Similarly, although through different biochemical mechanisms, the observed decrease of APP levels could also represent another pathway through which low-dose brain radiation could be employed as a tool to reduce the biochemical substrates of *β*-amyloid plaques and consequently reduce the related toxic effects[45].

Importantly, these new findings need to be confirmed in terms of safety and long-term efficacy by using different types of animal experiments and clinical trials in humans. Some clinical trials employing radiation in the context of a specific neurodegenerative disorder such AD have been recently proposed and approved (https://clinicaltrials.gov).

If confirmed at a larger scale, these new experimental data could have a major clinical and societal impact for the use of low-dose brain radiation as new neuro-radiotherapeutic tool for different neurodegenerative conditions, including, but not limited to, tauopathies such as AD, progressive supranuclear palsy (PSP) and chronic traumatic encephalopathy (CTE).

Intriguingly, the hyperphosphorylation process of Tau (as measured, for example, by CP13 levels) is a process normally present during normal brain development, and it is one of the earliest events that occur during the pathogenesis of different neurodegenerative disorders[46]. Tau hyperphosphorylation is hypothesized to be a complex molecular mechanism whereby a single and then multiple amino acid sites across the entire amino acid sequence of the protein are consecutively and progressively hyperphosphorylated leading to abnormally high levels of insoluble pTau followed by its intracellular pathological accumulation ultimately affecting normal neuronal and non-neuronal (e.g. glia) cellular functions[43,44]. In addition, our findings show that, at least three of the possible enzymes normally activated during Tau phosphorylation/dephosphorylation processes (GSK3*β,* pGSK*β* [*Y*216], PP2A- *βα)*,, remained unchanged after 4 weeks from the radiation time point in brain regions examined in this study. These data seem to suggest that both kinase and phosphatase enzymes could have reached a steady-state equilibrium in those examined regions at that specific post-radiation time point (4 weeks). Nonetheless, we cannot exclude that other phosphorylation/dephosphorylation enzymes or biochemical mechanisms might be involved in the interactions between pTau and the effects of radiation or that other chemical reactions (e.g. methylation) may occur.

Furthermore, our data show that lower levels of Ser202-phosphorylated-Tau (as detected by CP13 levels) in the FC and H regions were accompanied by concomitant lower levels of APP and GAP43 in the CRB. Intriguingly, a series of studies described close and complex interactions between APP and GAP43 in different regions of the rodent brain[47,48]. APP is the

precursor protein for 1–40 β-amyloid protein, one of the two proteins (pTau being the other), that pathologically accumulates (in the form of extracellular 1–42 β-neuritic plaques) in subjects diagnosed with AD and it has also been shown to interact with GAP43 in mechanisms of axonal generation and neuroplasticity[49]. On the other hand, GAP43 is a protein known to be involved in multiple structural and functional aspects of axonal formation during neosynaptogenic processes (during developmental period) and reparative neuronal mechanisms (during adult life)[50]. In our study, a decreased level of APP and GAP43 was unexpected, but it was even more surprising to observe a post-radiation effect in only the CRB. This latter finding may be related to the well-established notion that the CRB is one of the most resistant regions of the CNS to AD pathology in comparison to other regions of the brain (for example, the H or the FC). Remarkably, this AD-pathology resistance is maintained even during the late stages of the AD natural progression. The notion about the relative resistance of the CRB against the pathological accumulation of pTau and β-amyloid lesions has been attributed to some genetic or biological protective factor, which remains mostly unknown. If there are direct interactions between APP and GAP43 in the CRB and why this particular region of the CNS appears to be more susceptible to a low-dose of brain radiation compared to other brain regions such as H or FC remains elusive, and it represents a fascinating question deserving of future research efforts.

In general, the reduction of soluble levels of pTau, APP, and GAP43 across different mammalian brain regions could also be due to the terminal effects of more basic mechanisms associated with DNA (or RNA) damage or, alternatively, repair activities, especially in those regions of the mammalian brain more susceptible to radiation. In support of an early DNA radiation-induced activation, we did find an increased level of DNA-polymerase-β in the FC region. This is not so surprising since the FC is one of the latest neuroanatomical regions to ontogenetically and phylogenetically fully develop very late during the CNS maturation process due to its high level of circuital complexity and biological instability[51]. Importantly, though, DNA-polymerase-β is one of the enzymes involved in reparative processes and in various duplicative and reparative DNA mechanisms that could have been indeed triggered by low-dose brain radiation.

In contrast to the lower levels of pTau, APP, and GAP43 in FC, H and CRB regions, but consistent with previous clinical and experimental observations, the level of GFAP in the H was higher in RAD- vs. SH-animals. Furthermore, the increased level of GFAP in the H (as measured by WB quantifications) was confirmed by an initial by obvious process of astroglial cell reaction as detected at immunohistochemistry. More specifically, based on the immunohistochemistry-microscopic inspection, the astrogliosis seems to be localized at level of the peri-dental gyrus (peri-DG) area of the H (*Figure 6)* - one of the hippocampal subregions more often activated during various physiological and pathological processes affecting the H. WB and neuropathological findings suggest then the co-presence of an early neuroinflammatory response in the H associated with a reduction of other proteins levels (e.g. pTau) in the H itself and FC region. Furthermore, levels of IBA–1 (a marker of microglia) and MBP (a marker of myelin), did not differ in RAD- vs. SH-animals in any of the considered brain regions and no changes were observed at histological level or immunohistochemistry at high-magnification light microscopy inspection. These last findingssuggest that microglial cells and oligodendrocytes may possibly react at a later stage or at a much slower reacting rate compared to other possible more “radio-sensitive” cell types.

In general, the WB results obtained from low-dose radiation did not parallel any obvious brain lesion observable by histology stains (HE, LFB, CV) or immunohistochemistry, except for the increase of GFAP as a signal of astrogliosis in the H (*Figure 6)*.. We would like to emphasize that increased levels of GFAP are not necessarily linked to detrimental effects since astroglial cells are also involved in various regenerative and neurogenesis phenomena[52]. Moreover, the absence of immunohistochemistry-based histopathological brain lesions in RAD-vs. SH-animals indirectly confirmed the reduced levels of pTau, APP, and GAP43 across all the examined regions. In fact, those reduced levels of soluble proteins could have prevented the generation of the biochemical conditions necessary to determine molecular changes (e.g. increase levels of Tau, pTau/Tau ratio abnormalities) that are expected to induce the pathological accumulation of insoluble hyperphosphorylated-Tau in long-distance cortical neurons for example.

One of the major points of strength of this study is that we have used a large mammalian brain under normal anatomical and physiological conditions in order to observe possible molecular and neurohistopathological changes due to low-dose brain radiation after 4 weeks and that a compound like captopril is involved in those specific changes. These results in swine are

relevant since the swine brain represents a neural system that is much closer to humans than rodents in terms of neuroanatomy, neurocircuitry complexity, cerebro-vascular physiology, liver metabolism, pharmacology, etc. This makes swine brain an excellent model for brain radiation research while searching for its potential beneficial effects at molecular and behavioral level. These species-related considerations are especially important when considering that recent studies have shown that the gene responses to radiation (e.g. in the blood) vary greatly across different species[53].

To the best of our knowledge, these molecular and neuropathological findings observed 4 weeks following low-dose total-body radiation in a large mammalian brain are unique and of special relevance for possible future therapeutic applications to conditions affecting the CNS, especially those conditions associated with different types and mechanisms of misfolded protein accumulation. Future larger studies are necessary to precisely define other possible important brain-radiation effects and possible interacting or modifying factors such as minimally necessary effective total dose to administer, best fractionated scheme for each specific brain region and condition, definition of possible stereotactic approaches, genetic background-based response, and other factors not determined yet. Establishing all these parameters could greatly improve the beneficial and therapeutic applicability of low-dose brain radiation during the early phases of various neurodegenerative conditions in humans.

Materials And Methods

Animals

All animal handling procedures were in compliance with guidelines from the National Research Council for the ethical handling of laboratory animals and approved by the *(Affiliations Removed for Peer Review)* Institutional Animal Care and Use Committees. Male Gottingen minipigs ranging in age from ~6.0–6.5 months were purchased from Marshall Farms Group Ltd. USA (North Rose, NY, USA). All swine were kept in a barrier facility for animals accredited by the Association for Assessment and Accreditation of Laboratory Animal Care International. Swine were housed in pairs. Animal rooms were maintained at 21±2°C, 50±10% humidity, and 12-hour light/dark cycle with food and water available ad libitum. Swine were acclimatized to the animal facility for 3 days prior to the start of the study. Swine were divided into the following groups (total animal number was achieved over the course of 4 separate experiments):

1. Sham+Vehicle (*n*=4)
2. Radiation+Vehicle (*n*=6)
3. Sham+Captopril (*n*=6)
4. Radiation+Captopril (*n*=6)

Approximately two weeks after arrival, swine receiving total-body radiation were deeply anesthetized with Ketamine/Xylazine (4.4mg/kg–2mg/kg) and transported to the High Level Cobalt facility at *(Affiliations removed for Peer Review).* While under deep anesthesia, swine were positioned in supportive slings and exposed one at a time, bilaterally, to a target total body dose of 1.79 Gy of Cobalt (^{60}Co) radiation delivered at a dose rate of 0.485–0.502 Gy/min as previously described[53]. After radiation procedures, each animal was transported back to the animal facility for recovery. Swine assigned to the sham (SH) groups were also deeply anesthetized with Ketamine/Xylazine (4.4 mg/kg–2 mg/kg) in the animal facility but were not transported to the Cobalt facility. Treatment with either Captopril (C8856, Sigma-Aldrich, St Louis, MO, USA), dissolved in sterile water and mixed in yogurt) (10 mg/animal, PO, twice daily) or Vehicle (yogurt, PO, twice daily) began at 4 hours post-radiation or control equivalent and continued twice daily for 12–14 days.

Tissue Collection

Euthanasia was performed with an intracardial injection of Euthasol (4.5 ml/kg) and confirmed by lack of heartbeat. Each animal underwent necropsy procedures for the sampling of different organs (spleen, lung, liver, kidney, jejunum, skin, bone marrow - to be used by collaborators) as well as the collection of the entire brain and spinal cord.

Each brain was grossly inspected and longitudinally dissected across the median line of the corpus callosum to separate the two cerebral and cerebellar hemispheres. The left hemisphere of each animal was quick-frozen in chilled liquid isopentane on dry ice (destined for molecular analyses). Frozen brains were kept at –80^{o}C until use. The right hemispheres were placed in 10% buffered formalin for tissue fixation (for histological and immunohistochemistry purposes).

Protein Extraction and Western Blot (WB) Procedures

Frozen brains were warmed to –20^{o}C in a cryostat. Each left cerebral hemisphere was cut into 100µm thick sections and further microdissected into three main anatomical regions: frontal cortex (FC), hippocampus (H), and cerebellum (CRB). The dissections were guided by following the Gottingen Minipig Brain Atlas (https://www.cense.dk/miniswine_atlas).

Samples containing both gray (GM) and subjacent white matter (WM) from all animals and from each dissected neuroanatomical region (FC, H, CRB) were homogenized in glass dounce homogenizers with ice cold lysis buffer (1ml/100mg tissue), which contained the following: 50 mM Tris-HCl (pH 8), 1% Igepal, 150 mM NaCl, 1 mM EDTA, 1 mM PMSF, 1 mM NaF, 1:100 protease inhibitor cocktail (Sigma-Aldrich, P2714, St. Louis, MO, USA). All samples were centrifuged at 12,000g for 20 minutes and supernatants collected, aliquoted and frozen at –80°C. Total protein content from each brain region (FC, H, CRB) was determined using the Micro BCA assay (Thermo-Fisher Scientific, 23235, Waltham, MA, USA). 20µg of protein per sample, for all brain regions listed, were loaded on Novex Nupage 4–12% Bis-Tris Gels (Life Technologies, NP0329, Carlsbad, CA, USA) and were electrophoresed at 200V constant for 30 min. Gels were transferred to PVDF membranes using the iBlot2 dry transfer method (Life Technologies, IB21001, Carlsbad, CA, USA). Membranes were blocked in 5% milk in 1X TBST for 1 hr at room temperature (RT). The primary antibodies (see paragraph below) were diluted to the appropriate working concentrations in 5% milk in 1 X TBST and incubated on the membranes overnight at 4°C. Membranes were then rinsed 3x 5 min in TBST. Appropriate HRP tagged secondary antibodies (see paragraph below) were diluted 1:2000 in 5% milk in 1X TBST and incubated on the membranes for 1 hour at RT. Membranes were rinsed 3x 5 min in TBST and 1x 5 min in TBS. Membranes were incubated with chemiluminescent substrate (SuperSignal West Pico Chemiluminescent Substrate, Thermo-Fisher Scientific, 34577, Waltham, MA, USA) for 1 min and imaged on the LiCor C-Digit Blot Scanner (LiCor Biosciences, Lincoln, NE, USA). All membranes were stripped one time with Restore Plus Stripping Buffer (Thermo-Fisher Scientific, 46430, Waltham, MA, USA), for 10 min, rinsed with TBS and processed for immunoblotting as described above using GAPDH (1:40000, Millipore-Sigma, AB2302, Billerica, MA, USA) for the loading control. Densitometry was performed with NIH ImageJ software (2.0.0) with all protein signal intensities normalized to GAPDH signal intensity.

Primary antibodies for the targeted protein level changes targeted

To examine possible neuronal, astroglial, and microglial protein expression level changes occurring across the three selected brain regions (FC, H, CRB) in radiated (RAD)- vs. sham (SH)-animals four weeks after the radiation time-point, the following primary antibodies were used: CP13 (which recognizes Tau protein phosphorylated at amino acid serine in position 202 [Ser–202])[55] (1:250; this antibody was a gift of Professor Peter Davies, Albert Einstein College of Medicine, Bronx, NY, USA); HT7 (which recognizes all forms of Tau protein) (1:500; Thermo-Fisher Scientific, MN1000, Waltham, MA, USA); and an anti-β-tubulin antibody (1:5000; Thermo-Fisher Scientific, 322600, Waltham, MA, USA). Levels of HT7 and anti-β-tubulin antibody were measured to determine expression level changes of all Tau forms and possible corresponding associated changes in β-tubulin levels due to Tau interaction with tubulin molecules to stabilize microtubules[42]. In addition, we measured the expression levels of some kinase and phosphatase enzymes normally associated with the phosphorylation status of Tau by measuring the following: GSK3β(1:500; BD Biosciences, 610201, San Jose, CA, USA), a constitutively active kinase responsible for phosphorylation of Tau[56]; pGSK3β (Y216) (1:500; BD Biosciences, 612312, San Jose, CA, USA), a phospho-activated [Y216] kinase related to Tau[57,58]; and PP2A-$\beta\alpha$ (1:500; Millipore-Sigma, cat.#05–592, Billerica, MA, USA), a primary Tau phosphatase[59–60]. We also explored possible DNA damage/repair level changes by measuring DNA polymerase-β[61](1:1000; cat.#ab26343, Abcam, Cambridge, MA, USA).

We hypothesized that synapse-associated proteins could be altered in RAD- vs. SH-animals, so we also measured the expression levels of GAP43 (1:5000; cat.#ab232772, Abcam, Cambridge, MA, USA) - a marker associated with neosynaptogenesis, neuroplasticity, and axonal regeneration[62]. Furthermore, we measured expression levels of proteins known to be associated with longer term post-radiation effects (e.g. neuroinflammation, microglia activation, and demyelination) by measuring levels of glial fibrillary acidic protein (GFAP) (1:10000; Leica Biosystems, cat.#NCL-L-GFAP-GA5, Newcastle Upon Tyne, UK), a marker of astroglial cells[63], ionized calcium-binding adapter molecule 1 (IBA–1) (1:1000; cat.#ab178847, Abcam, Cambridge, MA, USA), a marker for microglial cells[64], and myelin basic protein (MBP) (1:2000; cat.#ab7349, Abcam, Cambridge, MA, USA), a marker of myelination[65]. Lastly, we measured levels of amyloid precursor protein (APP) (1:1000; Millipore-Sigma, cat.#MAB348, Billerica, MA, USA), a marker associated with diffuse axonal injury (DAI) and involved in the pathogenesis of Alzheimer's disease (AD)[66–69].

Secondary Antibodies: The following HRP tagged secondary antibodies were used: Goat anti-mouse (1:2000; cat.#ab97040, Abcam, Cambridge, MA, USA), Goat anti-rabbit (1:2000; cat.#ab97080, Abcam, Cambridge, MA, USA), Goat anti-rat (1:2000; cat.#ab97057, Abcam, Cambridge, MA, USA), and Rabbit anti-chicken (1:5000; cat.#AP162P, Millipore-Sigma, Billerica, MA, USA).

Neurohistologic and Immunohistochemistry Procedures

Tissue blocks from each animal were uniformly processed using an automated tissue processor (ASP 6025, Leica Biosystems, Nussloch, Germany). After tissue processing, each tissue block was embedded in paraffin and cut in a series of 20 5µm-thick consecutive sections. The first three sections were respectively selected for hematoxylin and eosin (H&E), Luxol fast blue (LFB) and Cresyl Violet (CV) stains, while the remaining sections were available for immunohistochemistry procedures. Immunohistochemistry procedures for each antibody on all dissected brain regions were performed using a Leica Bond III automated immunostainer with a diaminobenzidine chromogen detection system (DS9800, Leica Biosystems, Buffalo Grove, IL). The following antibodies were used: anti-phosphorylated Tau (CP13) (mouse antihuman monoclonal antibody, 1:2000, epitope retrieval time 10 minutes; this antibody was kindly donated by Dr. Peter Davies, Albert Einstein College of Medicine, New York City, NY); anti-all forms of Tau (HT7) (mouse antihuman monoclonal antibody, 1:150, epitope retrieval time 10 minutes, MN1000, ThermoScientific, Waltham, MA, USA); anti-amyloid precursor protein (APP) (mouse antihuman monoclonal antibody clone 22c11, 1:10, epitope retrieval time 10 minutes, MAB348, EMD Millipore, Burlington, VT, USA); anti-glial fibrillary acidic protein (GFAP) (mouse antihuman monoclonal antibody GA5, 1:250, with bond heat-induced epitope retrieval, epitope retrieval time 10 minutes, PA0026, Leica Biosystems, Wetzlar, Germany); anti-ionized calcium-binding adapter molecule 1 (IBA–1) (rabbit polyclonal, 1:100, epitope retrieval time 10 minutes, Wako 016–20001, FUJIFILM Wako Pure Chemical Corporation, Osaka, Japan); and anti-myelin basic protein (MBP) (mouse monoclonal antibody, 1:100, MBP101, ab62631, Abcam, Cambridge, MA, USA).

All stained sections were scanned by an Aperio scanner system (Aperio AT2 - High Volume, Digital whole slide scanning scanner, Leica Biosystems, Inc., Richmond, IL) and stored in Biolucida system, a hub for 2D and 3D image data (version 2017, MBF Bioscience, Williston, VT, USA) for further assessment and analyses to verify the immunoreactivity (IR) for each antibody and histological distribution of possible lesions and their severity across all examined brain regions and conditions. A preliminary neuropathologic assessment for each section, region and animal was performed using Aperio ImageScope (Aperio ImageScope, version 2016, Leica Biosystems, Inc.). Compared to WB analyses, we examined more neuroanatomical regions for the immunohistochemistry evaluation: frontal cortex (FC), parietal and temporal cortex (PTC), basal ganglia (BG), hippocampus (H), occipital cortex (OC), cerebellum (CRB), and brainstem (BS). After a preliminary ImageScope inspection (max 20X), a Zeiss Imager A2 (ImagerA2 microscope, Zeiss, Munich, Germany) bright-field microscope inspection at higher magnification (40X, 63X oil-immersion objectives) was used to identify and digitally photograph possible histopathologic details as needed.

Statistics

A series of two-tailed unpaired *t*-tests were performed to verify if the administration of Captopril could have affected any of the protein expression levels considered in the study. These preliminary statistical analyses showed that no differences were present across all examined proteins between Vehicle- and Captopril-treated groups. Based on these analyses, both RAD- groups (RAD-Vehicle+RAD-Captopril) and both SH groups (SH-Vehicle+SH-Captopril) were pooled together. Thus, only the following two groups of animals were considered for the WB quantifications: RAD (n = 12) and SH (n = 10 for FC and H; n = 7 for CRB). 3 CRB from the SH- group were used in other experiments and thus not available for these WB analyses.

For each soluble protein considered in the study, a series of separate two-tailed unpaired *t*-tests was performed between RAD- vs. SH- groups. Statistical significance for each measured protein expression level in each anatomical region (FC, H, CRB) examined was established when $p \leq 0.05$.

References

1. Berris, T. et al. Nuclear and radiological emergencies: Building capacity in medical physics to support response. *Phys Med.* 42:93-98 (2017). doi: 10.1016/j.ejmp.2017.09.117. Epub 2017 Sep 9.
2. Dainiak, N. Medical management of acute radiation syndrome and associated infections in a high-casualty incident. *J Radiat Res.* 1;59(suppl_2):ii54-ii64. (2018). doi: 10.1093/jrr/rry004.
3. S. Food & Drug Administration. Radiological and nuclear emergency preparedness information from FDA, https://www.fda.gov/EmergencyPreparedness/Counterterrorism/MedicalCountermeasures/MCMIssues/ucm602102.htm?utm_campaign=20180329%20MCMi&utm_medium=email&utm_source=Eloqua#mcms (2018).
4. Theis, V.S., Sripadam, R., Ramani, V., Lal, S. Chronic radiation enteritis. *Clin Oncol (R Coll Radiol).* 22(1):70-83 (2010). doi: 10.1016/j.clon.2009.10.003. Epub 2009 Nov 7.
5. Akleyev, A.V. Normal tissue reactions to chronic radiation exposure in man. *Radiat Prot Dosimetry* 171(1):107-16 (2016). doi: 10.1093/rpd/ncw207. Epub 2016 Jul 29.
6. Prasanna, P.G. et al. Radiation-induced brain damage, impact of Michael Robbins' work and the need for predictive biomarkers. *Int J Radiat Biol*. 90(9):742-52 (2014). doi: 10.3109/09553002.2014.925607. Epub 2014 Jun 25.
7. Smart, D. Radiation Toxicity in the Central Nervous System: Mechanisms and Strategies for Injury Reduction. *Semin Radiat Oncol*. 27(4):332-339 (2017). doi: 10.1016/j.semradonc.2017.04.006. Review.
8. Shuboni-Mulligan, D.D. et al. Radiation chronotherapy-clinical impact of treatment time-of-day: a systematic review. *J Neurooncol*. 145(3):415-427 (2019). doi: 10.1007/s11060-019-03332-7. Epub 2019 Nov 15.
9. Andrews, D.W. et al. Whole brain radiation therapy with or without stereotactic radiosurgery boost for patients with one to three brain metastases: phase III results of the RTOG 9508 randomised trial. *Lancet* 363:1665–1672 (2004).
10. Roberge, D., Petrecca, K., El Refae, M., Souhami, L. Whole-brain radiotherapy and tumor bed radiosurgery following resection of solitary brain metastases. *J Neurooncol*. 95:95–99 (2009).
11. Emami, B. et al. Tolerance of normal tissue to therapeutic radiation. *Int J Radiat Oncol Biol Phys.* 21:109–122 (1991).
12. Lawrence, Y.R. et al. Radiation dose-volume effects in the brain. *Int J Radiat Oncol Biol Phys*. 76(3 Suppl):S20–S27 (2010).
13. Langley, R.E. et al.Radiation-induced apoptosis in microvascular endothelial cells. *Br J Cancer*. 75:666–672 (1997).
14. Greene-Schloesser, D. et al. Radiation-induced brain injury: A review. *Front Oncol*. 2:73 (2012).
15. Burger, P.C., Mahley, M.S., Dudka, L., Vogel, F.S. The morphologic effects of radiation administered therapeutically for intracranial gliomas: A postmortem study of 25 cases. *Cancer* 44(4): 1256–1272 (1979).
16. Julow, J., Slowik, F., Kelemen, J., Gorácz, I. Late post-radiation necrosis of the brain. *Acta Neurochir. (Wien)*. 46(1-2):135-50 (1979).
17. Schiffer, D. et al. Radio- and chemotherapy of malignant gliomas. Pathological changes in the normal nervous tissue. *Acta Neurochir. (Wien).* 58(1-2):37-58 (1981).

18. Rubin, P., Gash, D.M., Hansen, J.T., Nelson, D.F., Williams, J.P. Disruption of the blood-brain barrier as the primary effect of CNS radiation. *Radiother Oncol*. 31(1):51-60 (1994)
19. Kim, S. et al. Neuroprotective and Anti-Inflammatory Effects of Low-Moderate Dose Ionizing Radiation in Models of Alzheimer's Disease. *Int J Mol Sci*. 21(10):3678 (2020). Published 2020 May 23. doi:10.3390/ijms21103678
20. Wilson, G.D. et al. Low Dose Brain Radiation Reduces Amyloid-β and Tau in 3xTg-AD Mice. *J Alzheimers Dis*. 75(1):15-21 (2020). doi:10.3233/JAD-200030
21. Douw, L. et al. Cognitive and radiological effects of radiotherapy in patients with low-grade glioma: long-term follow-up. *Lancet Neurol*. 8(9):810-8 (2009). doi: 10.1016/S1474-4422(09)70204-2. Epub 2009 Aug 7.
22. Lee, W.H., Sonntag, W.E., Mitschelen, M., Yan, H., Lee, Y.W. Radiation induces regionally specific alterations in pro-inflammatory environments in rat brain. *J Radiat. Oncol. Biol. Phys.* 86:132–44 (2010).
23. Mizumatsu, S. et al. Extreme sensitivity of adult neurogenesis to low doses of X-radiation. *Cancer Res*. 63:4021-27 (2003).
24. Rola, R., et al. Radiation-induced impairment of hippocampal neurogenesis is associated with cognitive deficits in young mice. *Neurol*. 188:316–30 (2004).
25. Haldbo-Classen, L.et al. Long-term cognitive dysfunction after radiation therapy for primary brain tumors. *Acta Oncol*. 58:745-752 (2019) doi:10.1080/0284186X.2018.1557786
26. Klein, M. et al. Effect of radiotherapy and other treatment-related factors on mid-term to long-term cognitive sequelae in low-grade gliomas: a comparative study *Lancet*. 360:1361-1368 (2002). doi:10.1016/s0140-6736(02)11398-5
27. Goldsby, R.E. et al. Late-occurring neurologic sequelae in adult survivors of childhood acute lymphoblastic leukemia: a report from the Childhood Cancer Survivor Study. *Clin. Oncol.* 28(2):324-31 (2010).
28. Saad, S., Wang, T.J. Neurocognitive deficits after radiation therapy for brain malignancies. *J. Clin. Oncol*. 38:634–40 (2015).
29. Scoccianti, S. et al. Changes in neurocognitive functioning and quality of life in adult patients with brain tumors treated with radiotherapy. *Neurooncol*. 108:291–308 (2012).
30. Sasaki, T., Kodaka, F., Taniguchi, G., Nishikawa, T., Watanabe, M. Experiential auditory hallucinations due to chronic epileptic discharges after radiotherapy for oligoastrocytoma. *Epileptic Disord*. 15(2):188–192 (2013).
31. Lam, L.C.W., Leung, S.F., Chow, L.Y. Functional experiential hallucinosis after radiotherapy for nasopharyngeal carcinoma. *Neurol. Neurosurg. Psychiatry* 64(2): 259–261 (1988).
32. Pettorini, B.L. et al. Radiation-induced brain tumours after central nervous system radiation in child-hood: A review. *Childs Nerv. Syst.* 24(7):793–805 (2008).
33. Andrews, R.N. et al. White Matter is the Predilection Site of Late-Delayed Radiation-Induced Brain Injury in Non-Human Primates. *Res*. 191(3):217-231 (2019). doi: 10.1667/RR15263.1. Epub 2019 Jan 29.
34. Tanikawa, S. et al. Autopsy report of a late delayed radiation injury after a period of 45 years. *Neuropathology* 39(2):106-110 (2019). doi: 10.1111/neup.12528. Epub 2019 Jan 4.
35. Soto, Claudio, and Sandra Pritzkow. "Protein misfolding, aggregation, and conformational strains in neurodegenerative diseases." *Nature neuroscience* 21 (10) 1332-1340 (2018). doi:10.1038/s41593-018-0235-9
36. McCart, E.A. et al. Delayed Captopril Administration Mitigates Hematopoietic Injury in a Murine Model of Total Body Radiation. *Rep*. 9(1):2198 (2019). doi: 10.1038/s41598-019-38651-2.
37. DeTure, M.A., Dickson, D.W. The neuropathological diagnosis of Alzheimer's disease. *Neurodegeneration* 14(1):32 (2019). https://doi.org/10.1186/s13024-019-0333-
38. Marples, B. et al. Cranial radiation significantly reduces beta amyloid plaques in the brain and improves cognition in a murine model of Alzheimer's Disease (AD). *Oncol*. 118(1):43-51 (2016). doi: 10.1016/j.radonc.2015.10.019. Epub 2015 Nov 23.
39. Seibert, T.M. et al. Cerebral Cortex Regions Selectively Vulnerable to Radiation Dose-Dependent Atrophy. *Int J Radiat Oncol Biol Phys*. 97(5):910-918 (2017). doi:10.1016/j.ijrobp.2017.01.005

40. Andres-Mach, M., Rola, R., Fike, J.R. Radiation effects on neural precursor cells in the dentate gyrus. *Cell Tissue Res.* 331(1):251-262 (2008). doi:10.1007/s00441-007-0480-9
41. Whoolery, C.W. et al. Whole-Body Exposure to 28Si-Radiation Dose-Dependently Disrupts Dentate Gyrus Neurogenesis and Proliferation in the Short Term and New Neuron Survival and Contextual Fear Conditioning in the Long Term. *Radiat Res.* 188(5):532-551 (2017). doi:10.1667/RR14797.1
42. Kadavath, H. et al. Tau stabilizes microtubules by binding at the interface between tubulin heterodimers. *Natl. Acad. Sci.* USA. 112(24):7501-6 (2015). doi: 10.1073/pnas.1504081112. Epub 2015 Jun 1.
43. Wang, J., Xia, Y., Grundke-Iqbal, I., Iqbal, K. Abnormal hyperphosphorylation of tau: sites, regulation, and molecular mechanism of neurofibrillary degeneration. *Alz. Dis*. 33 Suppl. 1, S123-39 (2013).
44. Iqbal K, Grundke-Iqbal I. Alzheimer neurofibrillary degeneration: significance, etiopathogenesis, therapeutics and prevention. *J Cell Mol Med*. 12(1):38-55 (2008). doi:10.1111/j.1582-4934.2008.00225.
45. Sivanesan, S., Tan, A., Rajadas, J. Pathogenesis of Abeta oligomers in synaptic failure. *Curr Alzheimer Res*. 10:316-323 (2019). doi:10.2174/1567205011310030011
46. Hefti, M.M. et al. Tau Phosphorylation and Aggregation in the Developing Human Brain. J. Neuropathol. *Neurol.* 78(10):930-938 (2019). doi: 10.1093/jnen/nlz073.
47. Zhang, Y. et al. Growth-associated protein GAP-43 and L1 act synergistically to promote regenerative growth of Purkinje cell axons in vivo. *Natl. Acad. Sci. USA*. 102(41):14883-8 (2005).
48. Masliah, E., Mallory, M., Ge, N., Saitoh, T. Amyloid precursor protein is localized in growing neurites of neonatal rat brain. *Brain Res.* 593(2):323-328 (1992). doi:10.1016/0006-8993(92)91329-d
49. Mishra, R. et al. GAP-43 is key to mitotic spindle control and centrosome-based polarization in neurons. *Cell Cycle*. 7(3):348-57 (2008).
50. Holahan, M.R. A Shift from a Pivotal to Supporting Role for the Growth-Associated Protein (GAP-43) in the Coordination of Axonal Structural and Functional Plasticity. *Cell Neurosci*. 11:266 (2017). doi: 10.3389/fncel.2017.00266. eCollection 2017.
51. Kolb, B. et al. Experience and the developing prefrontal cortex. *Natl. Acad. Sci. USA*. 109 Suppl 2(Suppl 2):17186-17193 (2012). doi:10.1073/pnas.1121251109
52. Morrens, J., Van Den Broeck, W., Kempermann, G. Glial cells in adult neurogenesis. *Glia*. 60(2):159-174 (2012). doi:10.1002/glia.21247
53. Ghandhi, S.A., Smilenov, L., Shuryak, I. Pujol-Canadell, M., Amundson, S. Discordant gene responses to radiation in humans and mice and the role of hematopoietically humanized mice in the search for radiation biomarkers. *Rep*. 9, 19434 (2019) doi:10.1038/s41598-019-55982-
54. Moroni, M. et al. Hematopoietic radiation syndrome in the Gottingen minipig. *Res*. 176(1):89-101 (2011).
55. Buée, L., Bussière, T., Buée-Scherrer, V., Delacourte, A., Hof, P. Tau protein isoforms, phosphorylation and role in neurodegenerative disorders. *Brain Res. Brain Res. Rev*. 33:95-130 (2000).
56. Ishiguro, K. et al. Glycogen synthase kinase 3 beta is identical to Tau protein kinase I generating several epitopes of paired helical filaments. *FEBS Lett*. 325:167-72 (1993).
57. Cross, D., Alessi, D., Cohen, P., Andjelkovich, M., Hemmings, B. Inhibition of glycogen synthase kinase-3 by insulin mediated by protein kinase B. *Nature*. 378(6559):785-9 (1995)
58. Doble, B., Woodgett, J. GSK-3: tricks of the trade for a multi-tasking kinase. *Cell Sci*. 116:1175–1186 (2003).
59. Qian, W. et al. PP2A regulates Tau phosphorylation directly and also indirectly via activating GSK-3beta. *Alzheimers Dis*. 19:1221-9 (2010).
60. Sontag, E., Nunbhakdi-Craig, V., Lee, G., Bloom, G., Mumby, M. Regulation of the phosphorylation state and microtubule-binding activity of Tau by protein phosphatase 2A. *Neuron*. 17:1201-7 (1996).
61. Ray, S., Menezes, M., Senejani, A., Sweasy, J. Cellular roles of DNA polymerase beta. *Yale J. Biol. Med*. 86:463-469 (2013).

62. Benowitz, L. and Routtenberg, A. A membrane phosphoprotein associated with neural development, axonal regeneration, phospholipid metabolism and synaptic plasticity. *TINS*. 10(12):527-532 (1987)
63. Hatten, M., Liem, R., Shelanski, M., Mason, C. Astroglia in CNS injury. *Glia*. 4:233-243 (1991).
64. Donat, C., Scott, G., Gentleman, S., and Sastre, M. Microglial activation in traumatic brain injury. *Aging Neurosci.* 9:208 (2017).
65. Helson, L. Radiation-induced Demyelination and Remyelination in the Central Nervous System: A Literature Review. *Anticancer Res*. 38(9):4999-5002 (2018). doi: 10.21873/anticanres.12818.
66. Gentleman, S., Nash, M., Sweeting, C., Graham, D., Roberts, G. b-Amyloid precursor protein (b-APP) as a marker for axonal injury after head injury. *Lett*. 160:139-144 (1993).
67. Pierce, J., Trojanowski, J., Graham, D., Smith, D., and McIntosh, T. Immunohistochemical characterization of alterations in the distribution of amyloid precursor proteins and b-amyloid peptide after experimental brain injury in the rat. *Neurosci*. 16(3):1083-1090 (1996).
68. Sheriff, F., Bridges, L., Sivaloganathan, S. Early detection of axonal injury after human head trauma using immunocytochemistry for b-amyloid precursor protein. *Acta Neuropathol*. 87:55-62 (1994).
69. Van Den Heuvel, C. et al. Upregulation of amyloid precursor protein messenger RNA in response to traumatic brain injury: an ovine head impact model. *Neurol*. 159:441-450 (1999).

Figures

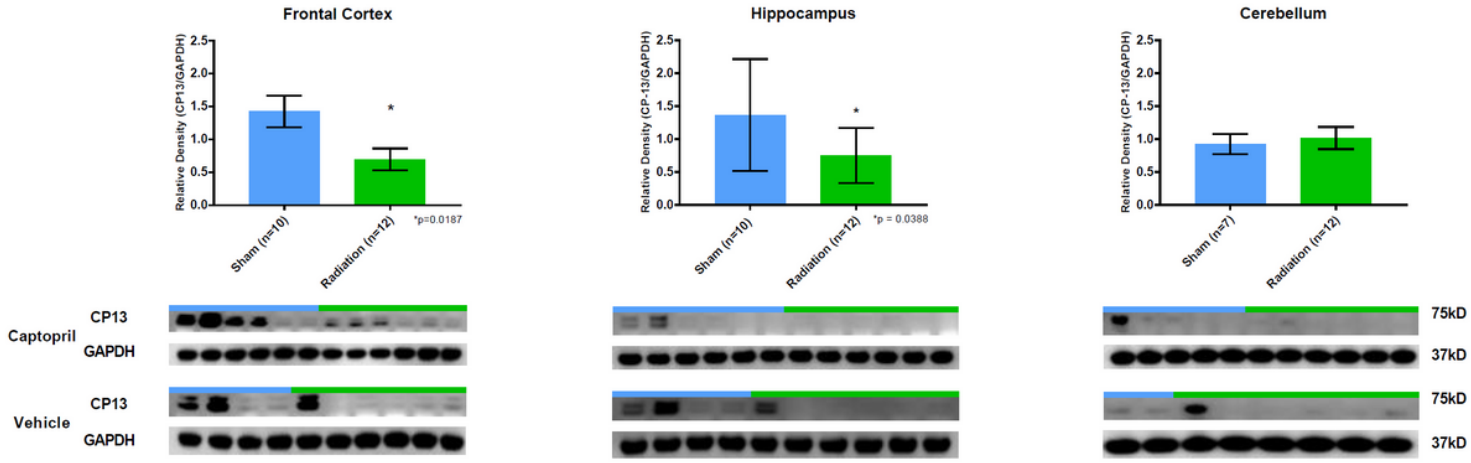

Figure 1

Phosphorylated-Tau expression in brain following total body radiation. Histograms representing the densitometric ratio of levels of pTau (CP13) with respect to GAPDH as measured in the frontal cortex, hippocampus and cerebellum in the brains of Gottingen mini-pigs 30-days after total body radiation (1.79 Gy of Cobalt [60Co]) with representative western blots# for sham and radiation exposed animals treated with Captopril or vehicle. There was no statistical difference between Captopril or Vehicle treated groups, so data was pooled for each group represented in histograms above. *indicates p values <0.05 as determined by 2-tailed, unpaired, t-tests. Error bars represent standard error of the mean (SEM). #for full length blots for each antibody, see Supplementary Fig. S5-S13

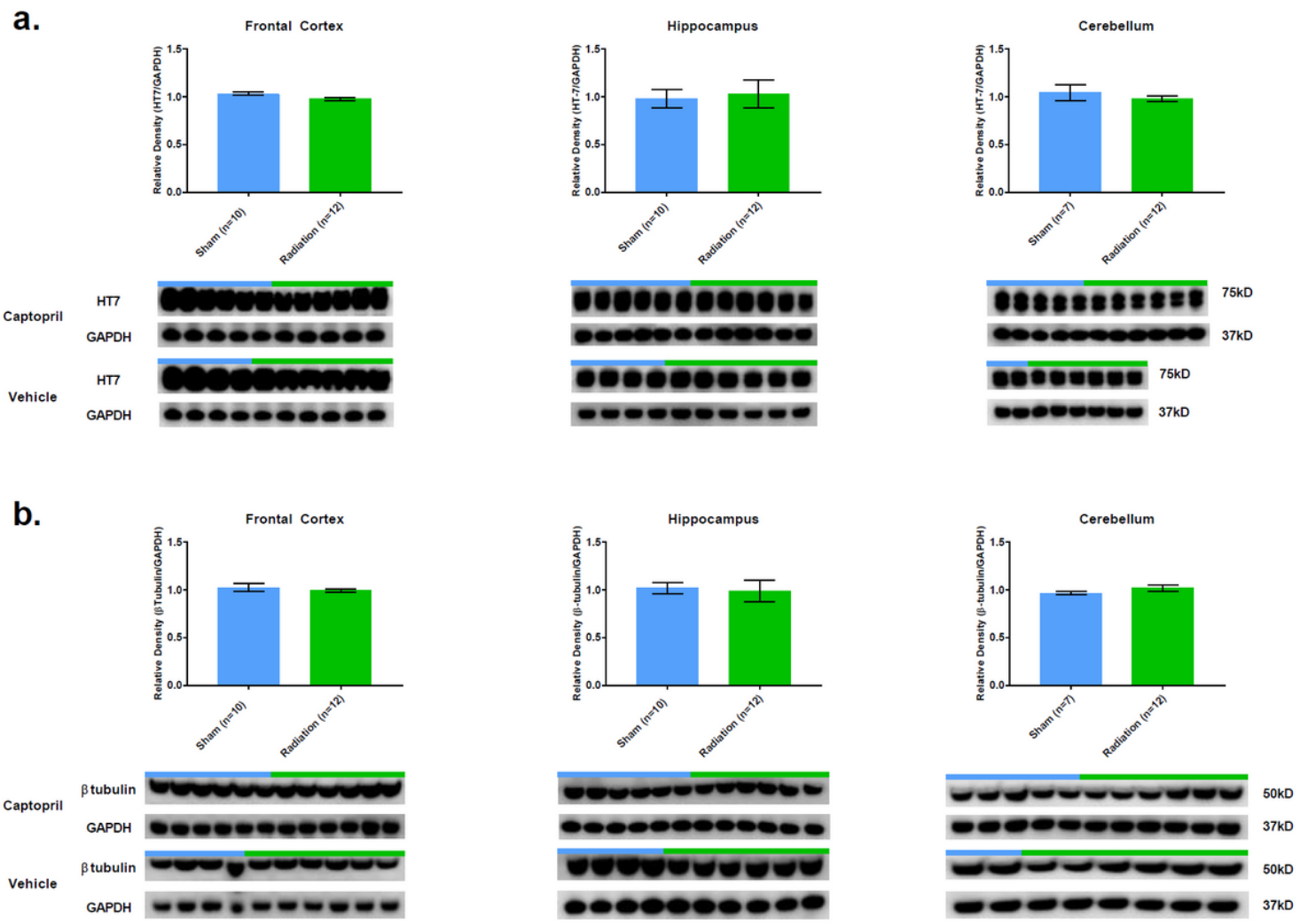

Figure 2

Phosphorylated-Tau expression in brain following total body radiation. Histograms representing the densitometric ratio of levels of pTau (CP13) with respect to GAPDH as measured in the frontal cortex, hippocampus and cerebellum in the brains of Gottingen mini-pigs 30-days after total body radiation (1.79 Gy of Cobalt [60Co]) with representative western blots# for sham and radiation exposed animals treated with Captopril or vehicle. There was no statistical difference between Captopril or Vehicle treated groups, so data was pooled for each group represented in histograms above. *indicates p values <0.05 as determined by 2-tailed, unpaired, t-tests. Error bars represent standard error of the mean (SEM). #for full length blots for each antibody, see Supplementary Fig. S5-S13

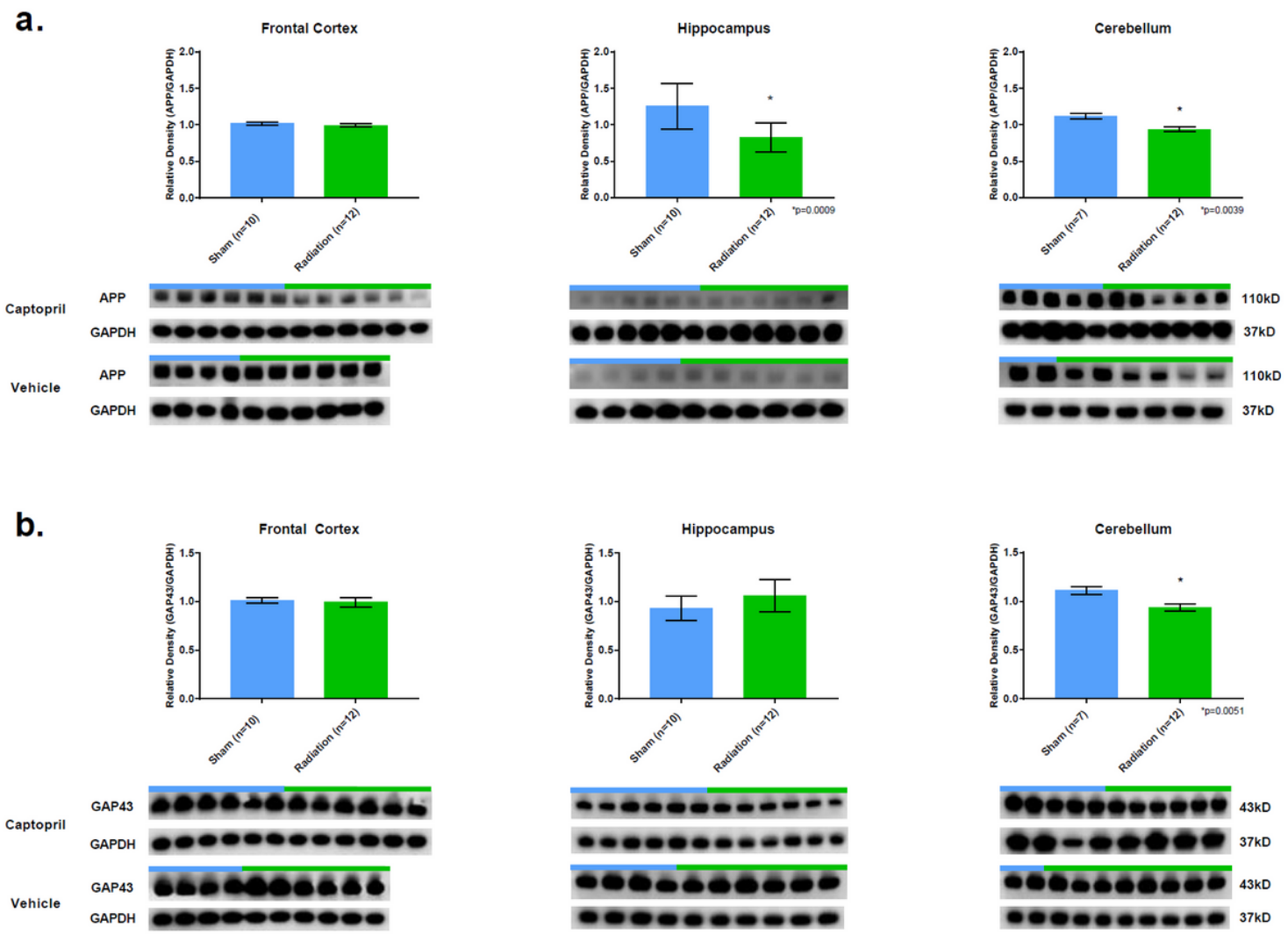

Figure 3

APP and GAP43 expression in brain following total body radiation. Histograms representing the densitometric ratio of levels of APP (A.) and GAP43 (B.) with respect to GAPDH as measured in the frontal cortex, hippocampus and cerebellum in the brains of Gottingen mini-pigs 30-days after total body radiation (1.79 Gy of Cobalt [60Co]) with representative western blots# for sham and radiation exposed animals treated with Captopril or vehicle. There was no statistical difference between Captopril or Vehicle treated groups, so data was pooled for each group represented in histograms above. * indicates p values <0.05 as determined by 2-tailed, unpaired, t-tests. Error bars represent standard error of the mean (SEM). #for full length blots for each antibody, see Supplementary Fig. S5-S13

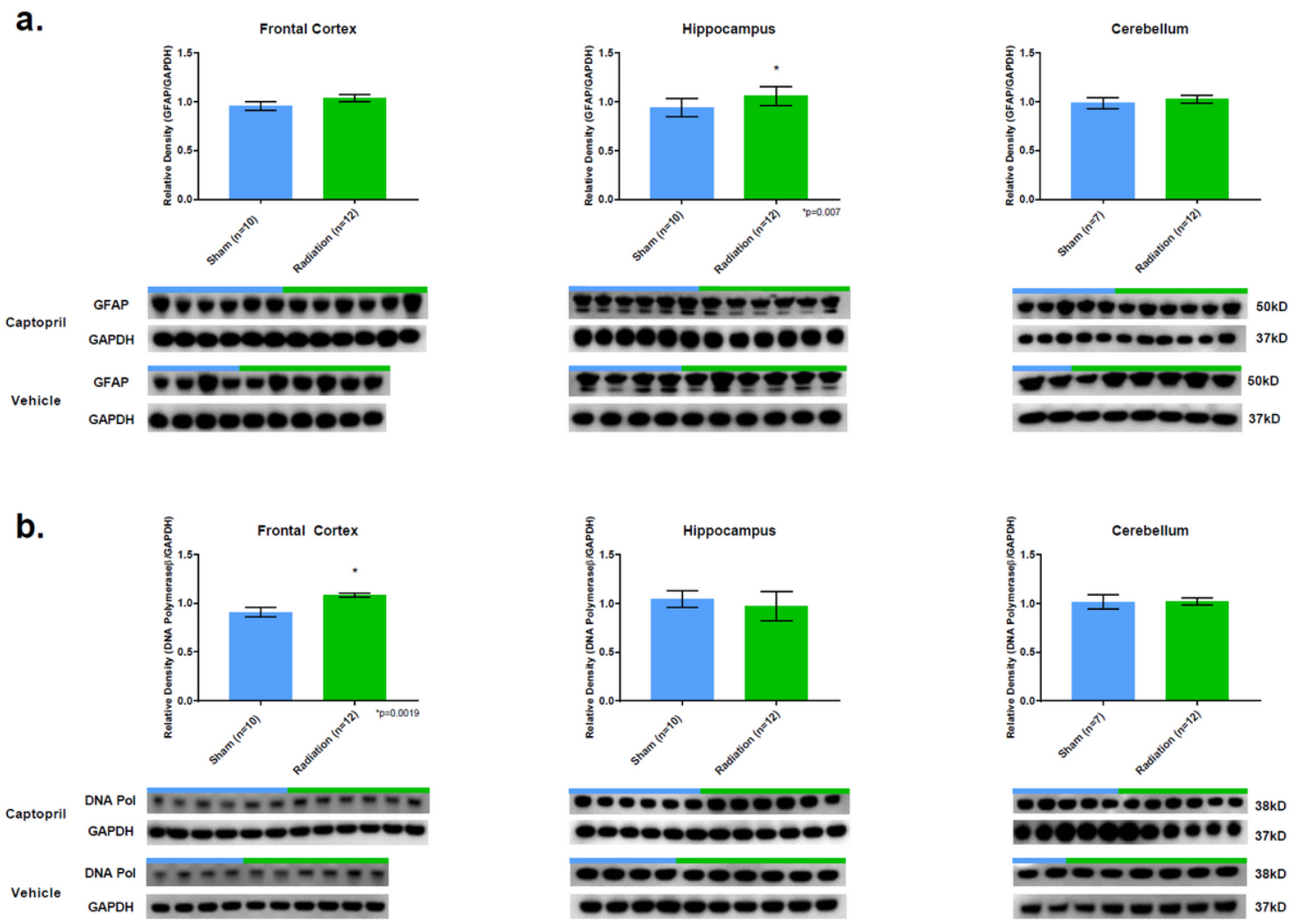

Figure 4

GFAP and DNA Polymerase-β expression in brain following total body radiation. Histograms representing the densitometric ratio of levels of GFAP (A.) and DNA polymerase-β (B.) with respect to GAPDH as measured in the frontal cortex, hippocampus and cerebellum in the brains of Gottingen mini-pigs 30-days after total body radiation (1.79 Gy of Cobalt [60Co]) with representative western blots# for sham and radiation exposed animals treated with Captopril or vehicle. There was no statistical difference between Captopril or Vehicle treated groups, so data was pooled for each group represented in histograms above. *indicates p values <0.05 as determined by 2-tailed, unpaired, t-tests. Error bars represent standard error of the mean (SEM). #for full length blots for each antibody, see Supplementary Fig. S5-S13

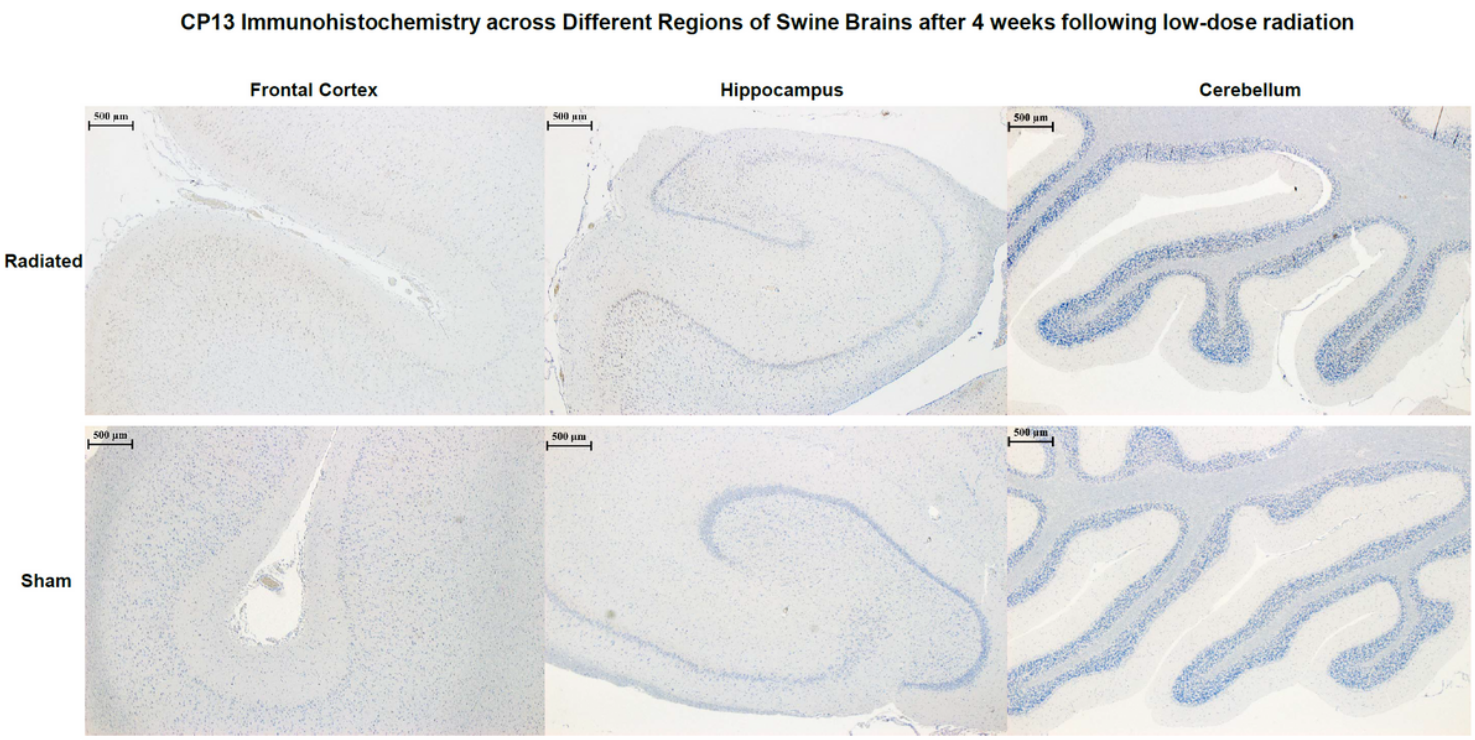

Figure 5

CP13 Immunohistochemistry across Different Regions of Swine Brains after 4 weeks following low-dose post-radiation. The figure shows Frontal Cortex, Hippocampus and Cerebellar Cortex of a Radiated and a Sham animal immunostained for pTau using CP13 antibody. To notice, no differences were present at histological level between Radiated vs. Sham animals across any of the anatomical region considered. The digital photographs were taken using a bright-light microscope (Zeiss ImagerA2) with a 20x objective.

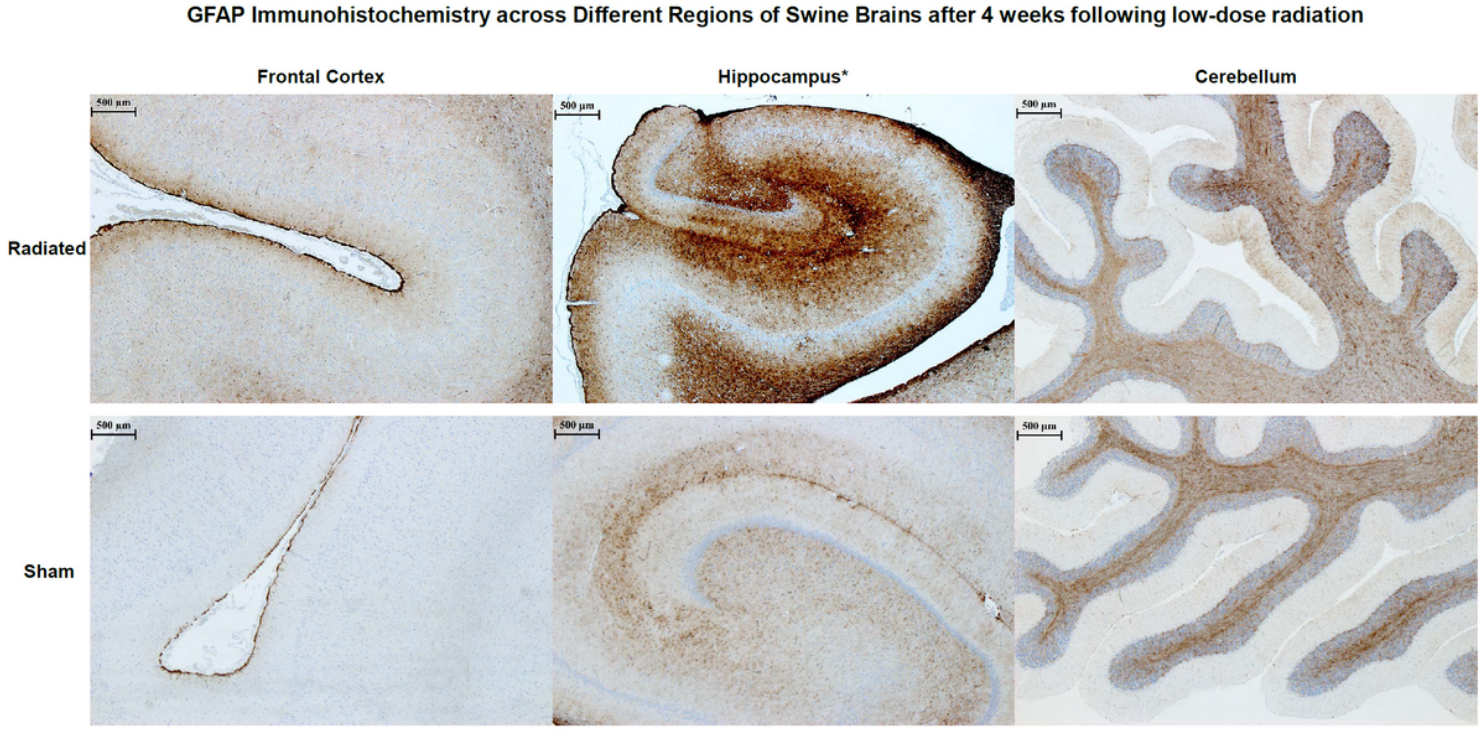

Figure 6

GFAP Immunohistochemistry across Different Regions of Swine Brain after 4 weeks following low-dose post-radiation. The figure shows Frontal Cortex, Hippocampus and Cerebellar Cortex of a Radiated and a Sham animal immunostained for glial fibrillary acidic protein (GFAP), a marker for astroglial cells. To notice the presence of the astroglial response in the Hippocampus (H), specifically in the peri-dental gyrus area, of the Radiated vs. Sham animal. The digital photographs were taken using a bright-light microscope (Zeiss ImagerA2) with a 20x objective.

Supplementary Files

This is a list of supplementary files associated with this preprint. Click to download.

- SupplementalFiguresforManuscript.pdf